Marine Geodesy, 27: 3–13, 2004

ISSN: 0149-0419 print / 1521-060X online
DOI: 10.1080/01490410490489313

Taylor & Francis
Taylor & Francis Group

An Illustration of the Contribution of the TOPEX/Poseidon—Jason-1 Tandem Mission to Mesoscale Variability Studies

P. Y. LE TRAON
G. DIBARBOURE

CLS Space Oceanography Division
Ramonville St. Agne, France

Almost one year of TOPEX/Poseidon (T/P) and Jason-1 data are processed to analyze the contribution of the tandem mission to mesoscale studies. To merge T/P and Jason-1 sea level anomaly (SLA) data, the main difficulty is to estimate consistent mean profiles for the two missions. An ocean variability correction is thus applied to T/P data before computing the mean profile. As a result, T/P and Jason-1 mean profile crossover differences are reduced from 4.6 cm to 1.5 cm rms only. Results from the tandem mission are then compared with those derived from Jason-1 alone and an external verification is performed with ERS-2 data. We show that, in regions with large mesoscale variability, the sea level and velocity can be mapped respectively with an accuracy of about 6% and 20 to 30% of the signal variance. Compared to Jason-1 or T/P, the tandem mission is also shown to provide a much better description of the Gulf Stream meanders and eddies and of their associated velocity field. These results are very encouraging and demonstrate the potential of an optimised two-satellite constellation for the mesoscale circulation monitoring.

Keywords altimetry, mesoscale, velocity, merging techniques

1. Introduction

The ocean circulation is dominated by mesoscale variability: eddies, meanders, rings, filaments, waves, fronts are observed almost everywhere in the ocean. Their energy exceeds that of the mean flow at least by an order of magnitude. Mesoscale variability can feedback energy on the mean flow and has a significant contribution to the total heat fluxes (e.g. Wunsch 1999; Roemmich and Gilson 2001). A better understanding of ocean circulation (including the large scale circulation and its role on climate) thus requires that we observe and model it at high space and time resolution to resolve the mesoscale variability (e.g. Wunsch 2001). This is also required for ecosystem modeling and for most of the operational oceanography applications (e.g. marine safety, pollution monitoring, offshore industry, fisheries).

Satellite altimetry has made a unique contribution to observing and understanding mesoscale variability (see Le Traon and Morrow 2001 for a recent review). Altimeter data analyses have provided a global description of the eddy energy and its seasonal/interannual variations. The time and space scales of the mesoscale circulation have been characterized.

Received 17 December 2003; accepted 7 March 2004.

This work was carried out by the CLS Space Oceanography Division as a contribution to the European Commission GAMBLE project.

Address correspondence to P. Y. Le Traon, CLS Space Oceanography Division, 8-10 Rue Hermès—Parc Technologique du Canal, 31526 Ramonville St. Agne. E-mail: pierre-yves.letraon@cls.fr

Satellite altimetry has also allowed a synoptic mapping of large eddies (e.g. Agulhas eddies) which is useful to better understand the role of eddies in transporting mass, heat, salt and nutrient. All these studies provide a good means of testing and validating models and theories.

Two altimeter missions at least are required to monitor the mesoscale variability (Koblinsky et al. 1992). This minimum requirement has been met since 1992 with the NASA/CNES TOPEX/Poseidon (T/P) and ESA ERS-1/2 altimeter missions and their successors Jason-1 and ENVISAT. Le Traon and Dibarboure (2002) (hereafter LD02) provide a recent summary of the mapping capabilities of the T/P+ERS (Jason-1+ENVISAT) configuration. Sea level can be mapped with an accuracy of less than 10% of the signal variance while the velocity can be mapped with an accuracy of 20 to 40% of the signal variance (depending on latitude). A large part of these errors are due to high frequency signals (periods $<$20 days). As a result, errors on 10-day averaged signals are smaller by a factor of 2 to 3. The contribution of the merging of T/P and ERS is also well illustrated by Ducet et al. (2000) and Ducet and Le Traon (2001). The velocity field was mapped globally; this yielded a characterization of the Eddy Kinetic Energy (EKE), anisotropy and eddy mean flow interactions with a resolution never achieved before.

Although the T/P+ERS merging has provided a much better representation of the mesoscale variability, it is far from fully resolving the mesoscale variability (see discussions in Greenslade et al. 1997 and Tai 1998). For example, resolving scales larger than 100 km and 10 days would require an optimized constellation of at least three altimeters (Tai 1998) or the use of swath techniques such as the Wide Swath Ocean Altimeter proposed on board Jason-2 (Pollard et al. 2002). To improve further our understanding of mesoscale variability, we now need to observe it at higher space and time resolution.

The interleaved tandem T/P—Jason-1 mission was proposed with this idea in mind (Fu et al. 2003). Since mid-September 2002, TOPEX/Poseidon has been flying mid-way between two adjacent Jason-1 ground-tracks. This yields a track separation of 1.4° in longitude and doubles the spatial resolution that can be achieved from T/P and Jason-1 data alone. First results from the interleaved tandem mission will be presented here to demonstrate its potential for mesoscale variability studies.

2. Data Processing

2.1. Data

We used 32 cycles of T/P and Jason-1 data spanning the period from October 2002 to June 2003. The T/P and Jason-1 data sets are IGDR data distributed by AVISO. The following corrections were used: GOT99 tidal correction (Ray 1999), inverse barometer correction with a variable mean pressure from ECMWF, dry tropospheric correction from ECMWF, non parametric sea state bias for T/P and BM4 sea state bias for Jason-1, dual frequency ionospheric correction, solid earth and polar tides, radiometer wet tropospheric correction (see Vincent et al. 2003). ERS-2 Fast Delivery Products (FDP) were also used for validation purposes. All these altimeter data sets were adjusted onto Jason-1 (e.g. Le Traon and Ogor 1998) to remove inconsistencies among missions and to reduce orbit errors. We thus get consistent sea surface height (SSH) data for the different missions.

2.2. T/P Mean Profile Estimation

To extract the sea level anomalies (SLA) for the different missions, we need to remove a mean profile $\langle \mathrm{SSH} \rangle$ from the individual SSH measurements ($\mathrm{SLA} = \mathrm{SSH} - \langle \mathrm{SSH} \rangle$). The

mean profile (MP) contains the geoid signal but also the mean dynamic topography (MDT) over the averaging period. For Jason-1, we used a MP calculated over a 7 year period (1993–1999).

Only several months of T/P data are available since its orbit change. Therefore a raw T/P mean would not be consistent with the mean used for Jason-1. A specific processing was thus applied to T/P data to get a MP consistent with Jason-1 MP (see also Le Traon et al. 2003). SSALTO/DUACS SLA maps (MSLA) derived from the near real time merging of Jason-1, GEOSAT Follow On and ERS-2 data were thus used to correct T/P data for ocean variability. MSLA are relative to a 7-year mean (1993–1999). They were interpolated in space and time along the T/P tracks to yield corrected T/P SSH (SSH_c):

$$SSH_c = SSH - MSLA_{DUACS} = SSH - (SSH - \langle SSH \rangle_{7\text{-year}} + \varepsilon) = \langle SSH \rangle_{7\text{-year}} - \varepsilon$$

ε represents the MSLA mapping errors (due to the ocean variability not resolved by the SSALTO/DUACS maps and residual altimeter errors). The corrected T/P SSH were then averaged over time to yield a T/P mean profile $\langle SSH_c \rangle$ ($\langle SSH_c \rangle = \langle SSH \rangle_{7\text{-year}} - \langle \varepsilon \rangle$). In regions of high mesoscale variability, ε variance is about 10% of the signal variance. If we assume that ε is decorrelated for the different cycles (which is a reasonable assumption since ε mainly corresponds to small scale variability), $\langle \varepsilon \rangle$ variance should be well below 1% of the signal variance, i.e. of the order of 1 to 2 cm rms for a 30 cm rms signal.

A crossover adjustment was finally applied to remove (small) residual biases between the two MPs. The ocean variability correction provides a T/P MP mean which is much more consistent with the Jason-1 MP. Figure 1 shows the mean crossover differences (averaged over $4^\circ \times 4^\circ$ boxes) before and after the ocean variability correction. Before correction, the crossover differences mainly represent the changes in ocean circulation between the Jason-1 7 year mean and the T/P 8-month mean. This effect is almost perfectly corrected with the ocean variability correction. The crossover differences between T/P and Jason-1 MPs are thus reduced from 4.6 cm (before correction) to 1.5 cm rms (after correction). In high eddy energy regions (rms of SLA larger than 20 cm), the crossover differences are reduced from 13 cm to 1.8 cm rms only. There is now an excellent consistency between the Jason-1 and T/P MPs, and accordingly between T/P and Jason-1 SLAs. SLAs from the two missions can now be merged for mesoscale circulation studies. This would be clearly impossible without the ocean variability correction.

2.3. Mapping Technique

The mapping method detailed in Le Traon et al. (2003) was then used to merge the SLA data from the two altimeter missions. The method requires an a priori knowledge of the covariance of sea level and measurement errors. Sea level covariance functions were derived from an analysis of T/P and ERS data (see Le Traon et al. 2003). We used a white measurement noise of 3 cm for TP and Jason-1 data. In addition, a noise of 10% of the signal variance was used to take into account the small scale variability which cannot be mapped and should be filtered in the analysis. Long wavelengths errors (LWE) due to residual orbit errors but also tidal or inverse barometer errors and high frequency ocean signals (e.g. Tierney et al. 2000) were also taken into account. After several sensitivity studies, their a priori variance was assigned to 25 cm^2. Maps were finally calculated every week on a $1/3^\circ \times 1/3^\circ$ Mercator grid (i.e. same resolution in latitude and longitude that is approximately equal to 33 km times the cosine of latitude).

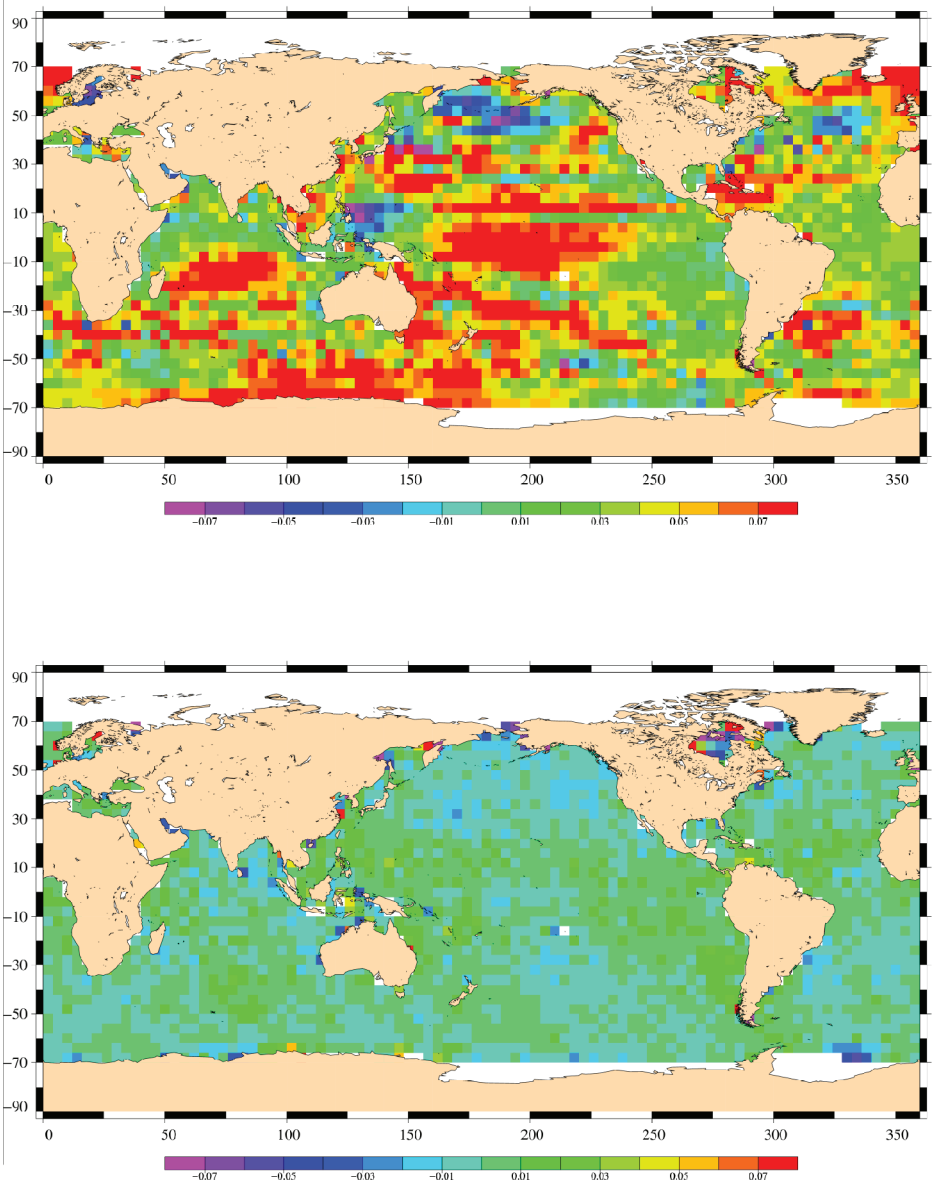

FIGURE 1 Mean of crossover differences between the T/P and Jason-1 mean profiles calculated over $4^\circ \times 4^\circ$ boxes before (upper figure) and after (lower figure) the ocean variability correction. Units are m.

3. Validation with ERS-2 Data

Sea level anomalies derived from the tandem mission and from Jason-1 alone were compared with all available ERS-2 along-track data over an 8-month time period (mid-October 2002 to early June 2003). ERS-2 SLA data were derived from ERS FDP data and using a mean profile computed from past ERS-1 and ERS-2 data (see Le Traon et al. 2003). ERS-2 data were then band-pass filtered using a Lanczos filter to retain wavelengths between 100 km

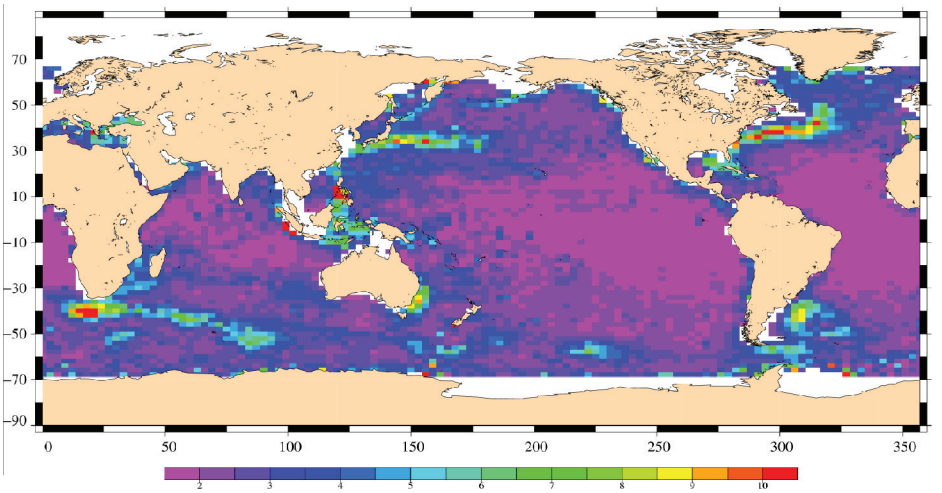

FIGURE 2 Rms error for the estimation of sea level along ERS-2 tracks from the tandem mission. Units are cm.

and 1000 km. Same processing was applied to the Jason-1 and tandem mission SLA data estimated along the ERS-2 tracks. This allows a reduction of altimeter noise and a removal of long wavelength errors (e.g. orbit error) while preserving most of the mesoscale signal.

Figure 2 shows the rms error for the estimation of sea level from the tandem mission along ERS-2 tracks. Figure 3 is given relative to the total sea level variance (estimated from ERS-2 data). In regions with large mesoscale variability, rms differences are comprised between 7 to 10 cm rms. For regions with a sea level variability larger than 20 cm rms, the sea level mapping error is about 6% of the signal variance. This is twice as small as the mapping error from Jason-1 data only. Note that these figures provide an upper bound of the mapping errors as they assume that ERS-2 data represent the truth. Apart for large mesoscale variability regions, errors are generally below 2 or 3 cm rms which shows that

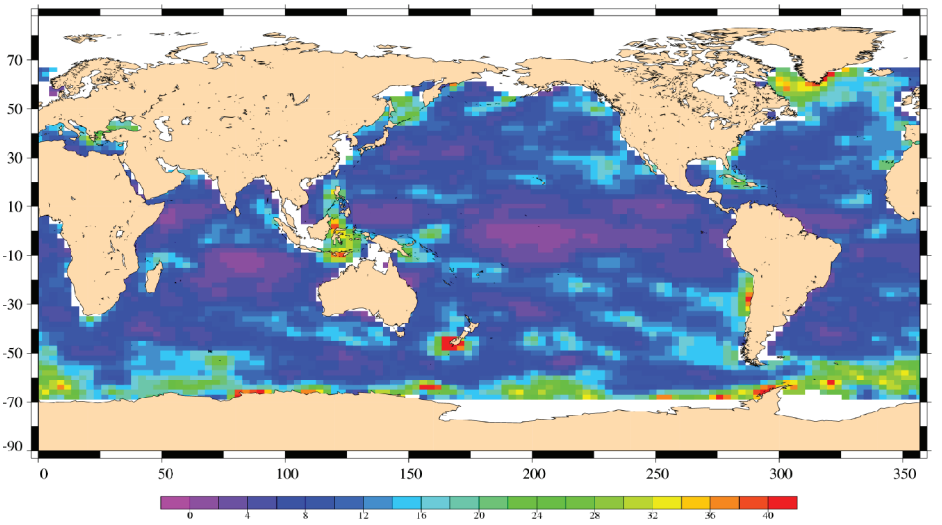

FIGURE 3 Rms error for the estimation of sea level along ERS-2 tracks from the tandem mission. Units are % of signal variance.

most of the signals (in the 100 km–1000 km wavelength band) observed along ERS-2 tracks are resolved by the tandem mission.

The same calculation was performed for the cross-track velocity. To compute cross-track velocities, more filtering of SLA data is needed to reduce the impact of altimeter noise. We used a filter cut-off wavelength that varies with latitude from 300 km at the equator to 100 km at 60°N/S. The cross-track velocity was then estimated from sea level gradients calculated over 14 km. If we assume a 4 cm white noise for ERS-2 FDP data (Dorandeu, personal communication), the noise on velocity estimation should be less than 4 to 5 cm/s (see Le Traon and Morrow 2001). Figure 4 shows the tandem mission velocity error variance, i.e. the variance of the difference between ERS-2 cross-track velocities and the tandem mission estimations. Figure 5 is given relative to the total velocity variance (estimated from ERS-2 data). For regions with sea level variability larger than 20 cm rms, the velocity mapping error from the tandem mission is comprised between 20 and 30% of the signal variance. This is again twice as small as with Jason-1 data alone. Note that errors are about 10–20 cm/s in high variability regions. In lower eddy energy regions, they range between 5 to 10 cm/s but the relative errors are larger (30 to 50% of the signal variance) as the velocity signals are much smaller.

These sea level and velocity mapping errors are consistent with theoretical estimates given in LD02. Note, however, that they do not include the effect of the small scales that were filtered out before the estimation of velocities.

4. Illustration of the Contribution of the Tandem Mission for Mesoscale Variability Studies

4.1. Monitoring of Gulf Stream Meanders and Eddies

Figure 6 provides an illustration of the potential of the tandem mission for a better monitoring of the eddy field. The absolute dynamic topography in the Gulf Stream region on December 11, 2002 derived from the combination of Jason-1 and T/P is shown on the upper left figure. A mean dynamic topography (Rio 2003) was added to the SLA data to get absolute dynamic

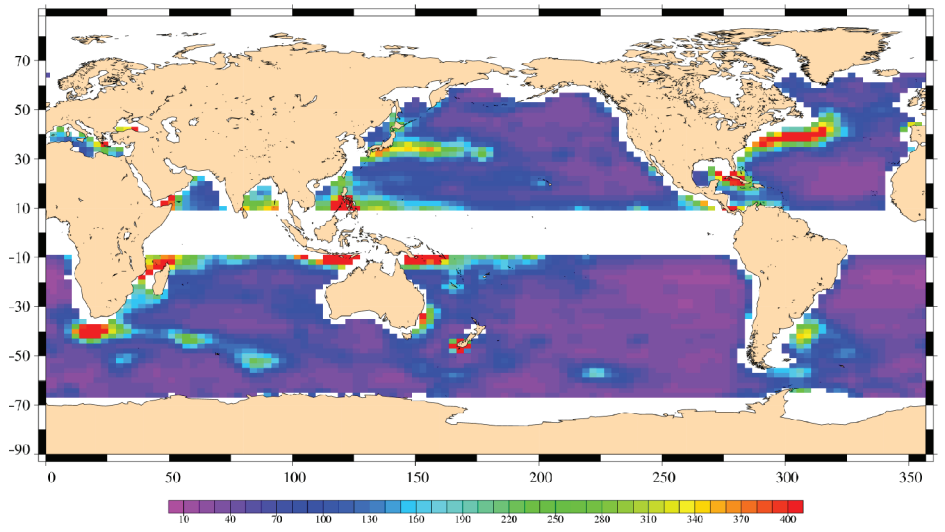

FIGURE 4 Error variance for the velocity estimation along ERS2 tracks from the tandem mission. Units are $(cm/s)^2$.

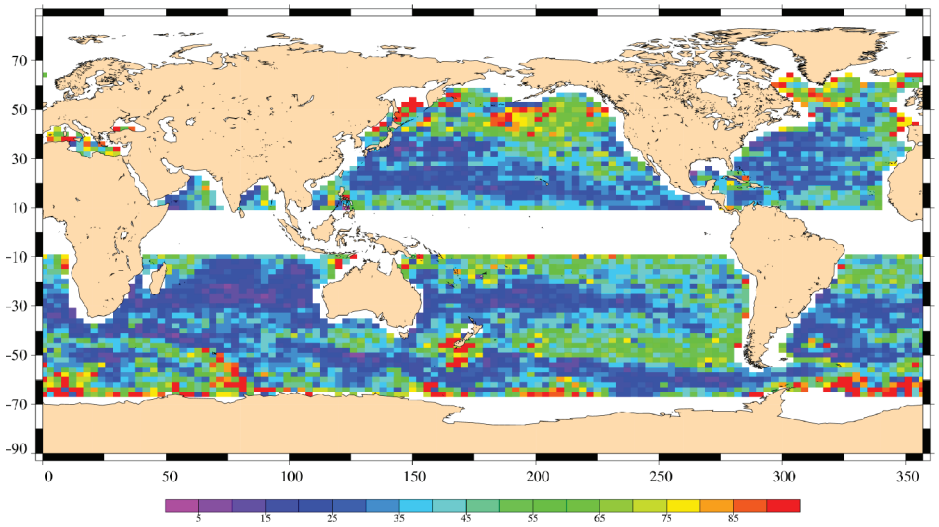

FIGURE 5 Error variance for the velocity estimation along ERS2 tracks from the tandem mission. Units are % of total velocity variance.

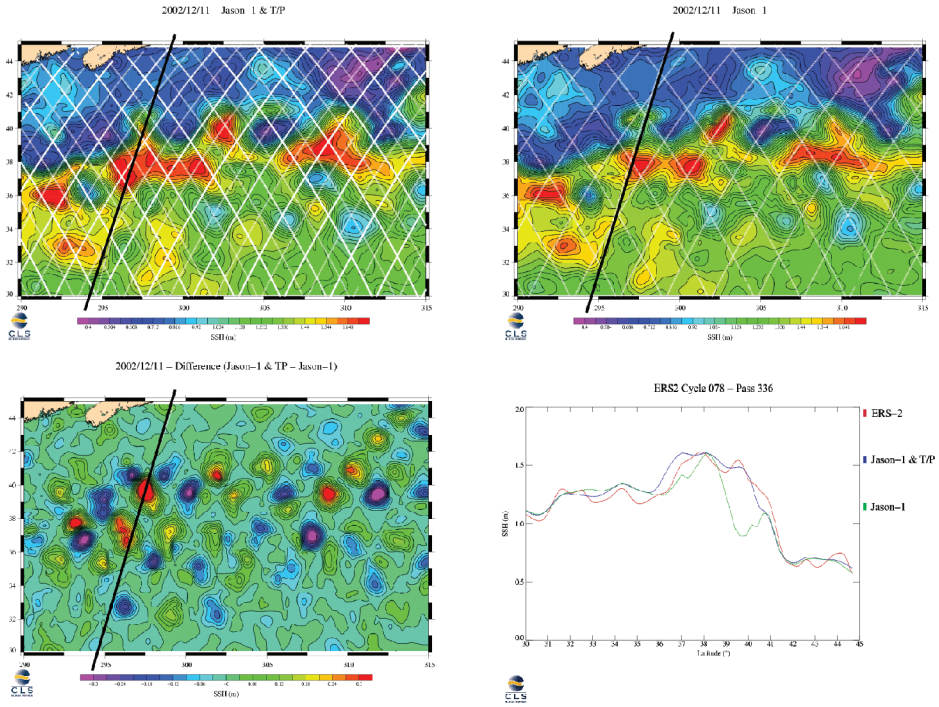

FIGURE 6 Absolute dynamic topography in the Gulf Stream region on December 11, 2002 derived from the combination of Jason-1 and TOPEX/Poseidon (T/P) (upper left figure). Jason-1 and T/P tracks are superimposed in white. The upper right figure is from Jason-1 data only. Lower left figure is the difference between the Jason-1+T/P and Jason-1 map. Comparison with the sea level observed along an ERS track (black track) (lower right figure).

topography. Jason-1 and T/P tracks are superimposed in white. The upper right figure is from Jason-1 data only. Lower left figure is the difference between the Jason-1+T/P and Jason-1 map. The Jason-1+T/P map provides a much better description of Gulf Stream eddies and meanders. Gradients are sharper and signals that are missed by the Jason-1 sampling (up to +/−40 cm) are well reproduced with the additional sampling from T/P.

This improvement is quantified through an external comparison with the sea level observed along an ERS-2 track (black track) (see previous section). The Jason-1+T/P map is able to reproduce most the signals observed by ERS (lower right figure) while the Jason-1 map failed to reproduce a Gulf Stream meander. The tandem mission maps are also much more consistent over time and allow us to monitor the temporal evolution of Gulf Stream eddies and meanders (see Figure 9).

4.2. Eddy Kinetic Energy and Velocity Mapping

Zonal (u') and meridonal velocity (v') maps were derived from Jason-1 and Jason-1+T/P sea level maps (through finite centred differences). From these maps, we then computed Eddy Kinetic Energy (EKE) ($EKE = 1/2\,(\langle u'^2\rangle + \langle v'^2\rangle)$). Figures 7 and 8 show respectively a monthly mean of EKE from Jason-1 and from the tandem mission. The picture we get from Jason-1 alone is, as expected, far from reality. Sampling effects are clearly visible. On the other hand, the path of the Gulf Stream is clearly seen on the EKE map derived from the tandem mission.

Same holds for the velocity field mapping. Figure 9 shows the absolute velocity field in the Gulf Stream region as derived from the tandem mission over six consecutive weeks. The MDT from Rio (2003) was used to reference the velocity anomalies. Thanks to its improved sampling, the tandem mission allows us to monitor the velocity field associated to the Gulf Stream meanders and eddies. The flow is almost continuous and we do not see any apparent artefact due to sampling effects. The accuracy of the mapped velocity field is about 10 to 20 cm/s which is much smaller than the observed velocities (maxima reaching 150 cm/s). The figure shows the formation and shedding of a cyclonic ring south of the Gulf Stream and the merging of two cyclonic rings in a recirculation cell south of the Gulf Stream.

One of the great advantages of the tandem mission is that it should allow us to map the two components of the velocity field with a similar accuracy (Le Traon and Dibarboure 2002). This is a clear improvement compared to T/P and ERS (or Jason-1 and ENVISAT) merging. One should thus be able to much better estimate Reynolds stresses, the anisotropy of the eddy field as well as eddy mean flow interaction. The time series is still too short to

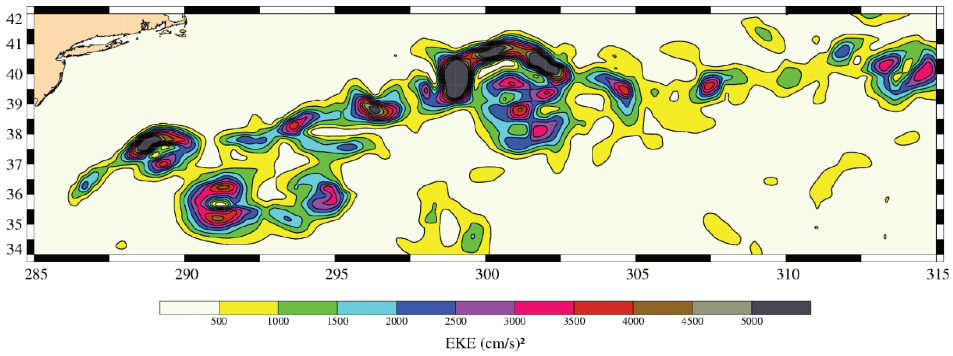

FIGURE 7 EKE for December 2002 derived from Jason-1 data. Units are $cm^2\ s^{-2}$.

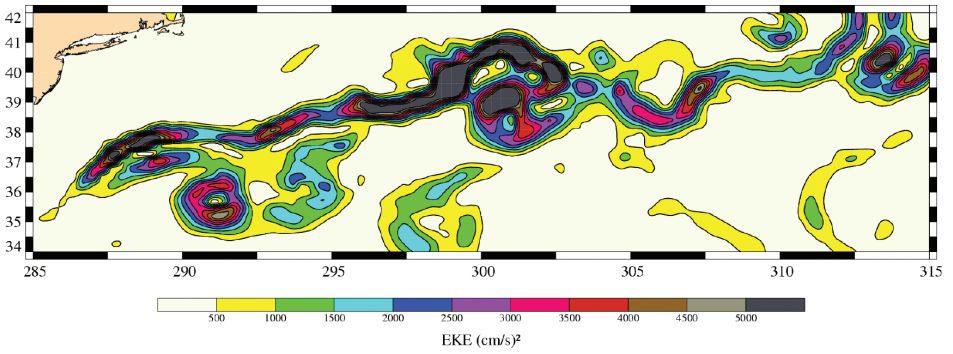

FIGURE 8 EKE for December 2002 derived from the tandem mission. Units are $cm^2\ s^{-2}$.

derive meaningful statistics and only global averages of the zonal and meridional velocity variances are shown here (Figure 10). They already show interesting characteristics such as the dominance of the zonal velocity variances in the equatorial and tropical regions, the larger zonal velocity variances in the Gulf Stream and Kuroshio regions and higher meridional velocity variances in the Brazil/Malvinas Confluence and Agulhas retroflection

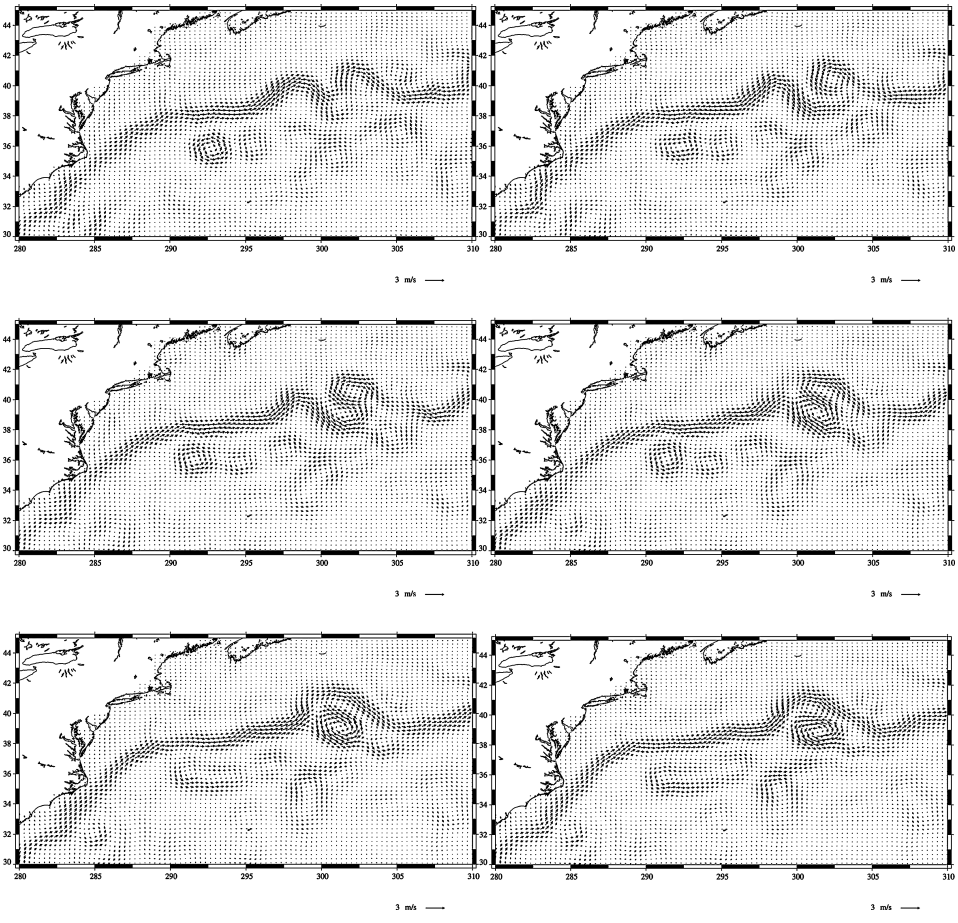

FIGURE 9 Snapshots of the absolute geostrophic velocities derived from the tandem mission from 2003/11/06 to 2003/12/11.

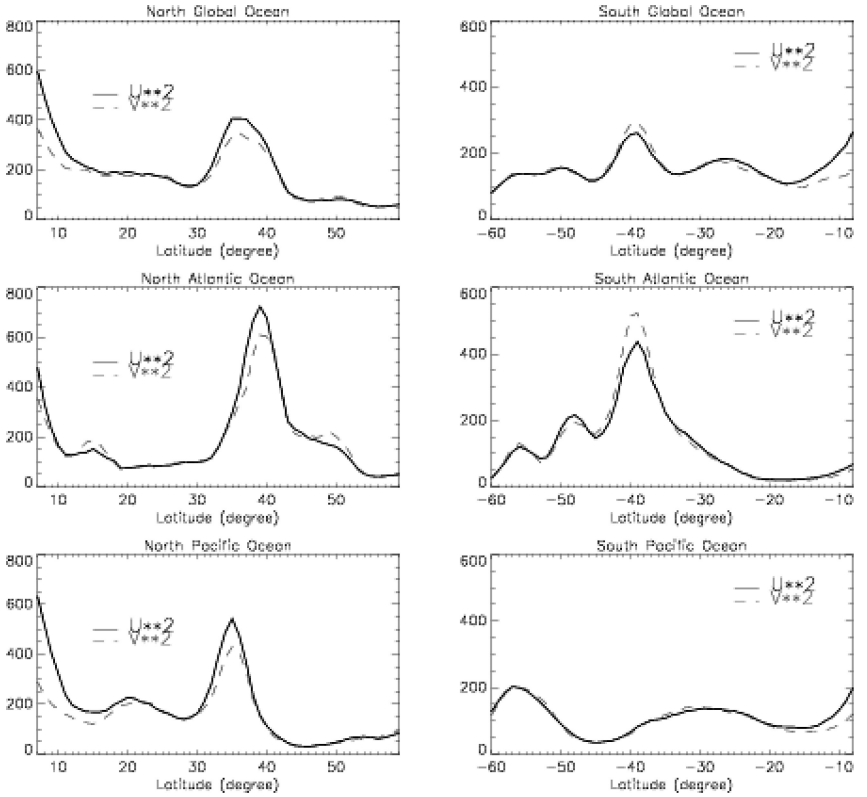

FIGURE 10 Zonally averaged zonal and meridional velocity variances derived from tandem mission sea level anomaly maps.

areas. Note that there is no apparent latitude effect in the estimation of the meridional and zonal velocity variances. With a longer time series, one should be able to derive maps of Reynolds stresses at high resolution that will provide new insights on flow anisotropy and eddy/mean interaction.

5. Conclusion and Perspectives

We have shown first that, thanks to a specific processing, it is possible to extract from the limited time series of T/P in its new orbit, T/P SLAs that are consistent with Jason-1 SLAs relative to a 7-year mean. Results from the merging of T/P and Jason-1 have then confirmed the potential of an optimized two satellite configuration for mesoscale variability studies. In regions with large mesoscale variability, the sea level and velocity can be mapped respectively with an accuracy of about 6% and 20–30% of the signal variance. This is a factor two less than the results derived from T/P or Jason-1 alone. Compared to Jason-1 or T/P, the tandem mission was also shown to provide a much better description of the Gulf Stream meanders and eddies and of their associated velocity field.

Future studies should now be performed over a longer time series and should focus on velocity analysis and eddy/mean flow interaction. Similar analyses should also be performed to analyze the contribution of the tandem mission together with GEOSAT Follow On and ERS-2/ENVISAT data. In addition to an improved understanding of the mesoscale variability, these analyses will provide useful inputs for the definition of future high resolution altimeter missions.

References

Ducet, N., P. Y. Le Traon, and G. Reverdin. 2000. Global high resolution mapping of ocean circulation from the combination of TOPEX/POSEIDON and ERS-1/2. *J. Geophys. Res.* 105:19,477–19,498.

Ducet, N., and P.-Y. Le Traon. 2001. A comparison of surface eddy kinetic energy and Reynold stresses in the Gulf Stream and the Kuroshio Current systems from merged TOPEX/Poseidon and ERS-1/2 altimetric data. *J. Geophys. Res.* 106:16603–16622.

Greenslade, D. J. M., D. B. Chelton, and M. G. Schlax. 1997. The Midlatitude resolution capability of sea level fields constructed from single and multiple satellite altimeter datasets. *J. Atm. Ocean. Tech.* 14:849–870.

Fu, L. L., D. Stammer, B. B. Leben, and D. B. Chelton. 2003. Improved spatial resolution of ocean surface topography from the TOPEX/Poseidon—Jason-1 tandem altimeter mission, EOS (in press).

Koblinsky, C. J., P. Gaspar, and G. Lagerloef. 1992. The future of spaceborne altimetry: Oceans and climate change, Joint oceanographic institutions incorporated, Washington, D.C., 75 pp.

Le Traon, P.-Y., and R. A. Morrow. 2001. Ocean currents and mesoscale eddies. Satellite Altimetry and Earth Sciences. A Handbook of Techniques and Applications, Academic Press ed. L.-L. Fu, and A. Cazenave (Eds.). Academic Press, 171–215.

Le Traon, P. Y., and G. Dibarboure. 2002. Velocity mapping capabilities of present and future altimeter missions: The role of high frequency signals. *J. Atm. Ocean. Tech.* 19:2077–2088.

Le Traon, P. Y., Y. Faugère, F. Hernandez, J. Dorandeu, F. Mertz, and M. Ablain. 2003. Can we merge GEOSAT Follow-On with TOPEX/POSEIDON and ERS-2 for an improved description of the ocean circulation? *J. Atm. Ocean. Tech.* 20:889–895.

Pollard, B., E. Rodriguez, L. Veilleux, T. Akins, P. Brown, A. Kitiyakara, M. Zawadski, S. Datthanasombat, and A. Prata. 2002. The Wide Swath Ocean Altimeter: Radar Interferometry for Global Ocean Mapping with Centimetric Accuracy, IEEEAC paper n° 068.

Rio. 2003. Combinaison de données in-situ, altimétriques et gravimétriques pour l'estimation d'une topographie dynamique moyenne globale. Phd thesis, Toulouse University, 260 pp.

Roemmich, D., and J. Gilson. 2001. Eddy Transport of Heat and Thermocline Waters in the North Pacific: A Key to Interannual/Decadal Climate Variability? *J. Phys. Ocean.* 31:675–688.

Tai, C. K. 1998. On the spectral ranges that are resolved by a single satellite in exact-repeat sampling configuration. *J. Atmos. Ocean. Technol.* 15:1459–1470.

Vincent, P., S. D. Desai, J. Dorandeu, M. Abalin, B. Soussi, P. S. Callahan, and B. J. Haines. 2003. Jason-1 Geophysical Performance Evaluation. *Marine Geodesy* 26:167–186.

Wunsch, C. 1999. Where do ocean eddy heat fluxes matter? *J. Geophys. Res.* 104:13235–13250.

Wunsch, C. 2001. Global problems and global observations, in Ocean Circulation and Climate: Observing and Modelling the Global Ocean, pp. 47–58, Academic Press, San Diego, CA.